Available online at www.sciencedirect.com

SCIENCE DIRECT®

International Communications in Heat and Mass Transfer 32 (2005) 539–547

International Communications in HEAT and MASS TRANSFER

www.elsevier.com/locate/ichmt

Modeling of a continuous fluidized bed dryer using artificial neural networks☆

S. Satish, Y. Pydi Setty*

Department of Chemical Engineering, National Institute of Technology, Warangal, India

Available online 19 December 2004

Abstract

The work involves experimentation on drying of solids in a continuous fluidized bed dryer covering different variables like bed temperature, gas flow rate, solids flow rate and initial moisture content of solids. The data are modeled using artificial neural networks. The results obtained from artificial neural networks are compared with those obtained using Tanks-in-series model. It was found that results obtained from ANN fit the experimental data more accurately compared to the RTD model with less percentage error. This indicates a better fit of artificial neural networks to experimental data compared to various mathematical models.

Keywords: Fluidized bed drying; Modeling; Artificial neural networks; Residence time distribution

1. Introduction

When a wet solid is subjected to thermal drying, two processes occur simultaneously:

1. Transfer of energy from the surrounding environment to evaporate the surface moisture.
2. Transfer of internal moisture to the surface of the solid and its subsequent evaporation due to process 1.

In process 1, the removal of water from the surface as vapor depends on the external conditions of temperature, air humidity and flow, area of exposed surface. In process 2, the movement of moisture

☆ Communicated by A.R. Balakrishnan.

* Corresponding author. Tel.: +91 870 245 9191x2611; fax: +91 870 245 9547.
E-mail address: psetty@nitw.ernet.in (Y. Pydi Setty).

0735-1933/$ - see front matter
doi:10.1016/j.icheatmasstransfer.2004.06.005

internally inside the solid is a function of the physical nature of the solid, its moisture content and the bed temperature.

The advantages offered by fluidized bed drying technology compared to other drying methods are principally as follows :

1. by rapid exchange of heat and mass between gas and particles, overheating of heat-sensitive particles is avoided.
2. heat transfer rates between fluidized bed and the immersed objects are high.
3. rapid mixing of solids leads to nearly isothermal conditions throughout the fluidized bed and thus reliable control of the drying process can be achieved easily.

Several mathematical models have appeared in the literature describing the RTD of solids in a continuous fluidized bed . The outlet moisture content of solids in a continuous fluidized bed dryer can be predicted using any of these models. Lenin Babu and Pydi Setty [1] reported the development of a drying kinetic model for a continuous fluidized bed dryer using Tanks-in-series model to predict average moisture content of solids. Such models obtained are based on the parameters like constant drying rate, critical moisture content and equilibrium moisture content that are characteristics of the solids obtained from the batch drying curve. These parameters exhibit a dependency on the system variables such as holdup of solids, diameter of the fluidization column, etc. Existing empirical equations defining the dependency relationships are specific to materials and to the batch drying operation. Little information is available in the literature on the empirical equations defining these relationships for the continuous drying operation.

Hence, the potential of Artificial Neural Networks as universal approximators can be explored and their usefulness in predicting the values of process performance variables from independent variables based on experimental continuous fluidized bed dryer data can be studied. For complex processes like fluidized bed drying, neural networks perform better than empirical models with noisy or incomplete information. Neural networks have a better filtering capacity than empirical models because of the microfeature concept, as each node encodes only a microfeature of the overall input–output pattern. The concept of microfeature implies that each node affects the input–output pattern only slightly. Only when all the nodes are assembled together into a single coordinated network do these microfeatures map the macroscopic input–output pattern.

2. Experimental setup and procedure

The experimental setup consists of a fluidization column made up of iron provided with a perforated plate of 3 mm perforations arranged with 6 mm triangular pitch. The plate acts as a distributor for air. It is provided with a downcomer weir. The distributor plate is provided with a vertical baffle of 90 mm in height and 20 mm in width. Wet solids are fed continuously through a hopper. The hopper is provided with a horizontally sliding perforated plate. The perforations are calibrated for solids flow rate. Air drawn from a compressor passes through a rotameter and then through an air chamber, which lies below the fluidization column. The rotameter measures the air flow rate. A heating coil provided along the outside surface of the fluidization column supplies necessary heat to the column. The coil is connected to a variac which in turn is connected to an electrical source. Temperatures at the center of the column and at the inner surface of the column are read directly from the temperature indicator using Copper–Constantan thermocouples attached

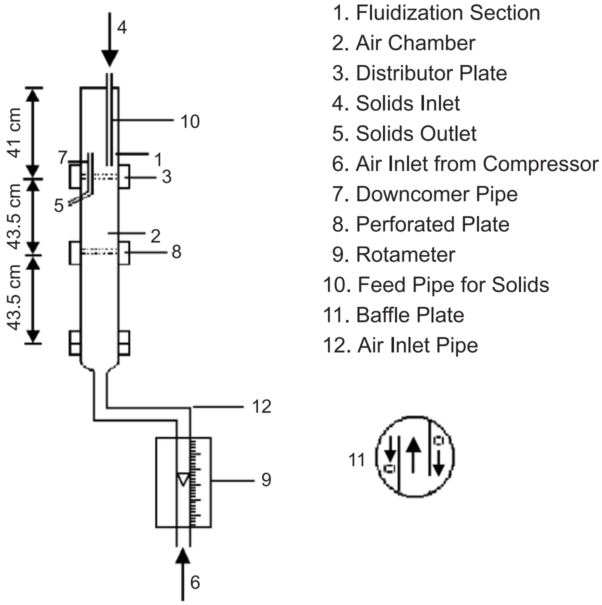

Fig. 1. Experimental setup.

to it. The temperature indicator is pre-calibrated for temperature correction using a thermometer. The variac provides constant supply of heat to the column to maintain constant required temperature within the column throughout the experiment.

The solids fed at one end of the column fluidize in the presence of upflowing air and move around the baffle and finally exit through the downcomer weir at the other end of the column and in the process the solids get dried. The other end of the downcomer protrudes through the air chamber to outside and the samples were collected at different time intervals at steady state. The samples were then analyzed for moisture content. The weight of moisture removed and that of dry sand were determined by weighing

Table 1
Experimental conditions

Inside diameter of the column, mm	89.0
Thickness of the column, mm	2.00
Downcomer diameter, mm	10.00
Length of the column, mm	1280.00
Bed height, mm	30.00
Mass flow rate of solids, kg/m^2-s	0.29–0.67
Mass flow rate of air, kg/m^2-s	1.08–1.90
Temperature at the centre of the column, °C	35–60
Initial moisture content of solids, kg moisture/kg dry solid	0.015–0.032

Particle characteristics

Sample	Binary solid mixture
Density, kg/m^3	2620
Diameter, mm	0.83

Table 2
Experimental data on drying of solids [2]

t	c(t)	t	c(t)
150	0.001251	255	0.000932
165	0.001201	270	0.000844
180	0.001096	285	0.000784
195	0.001081	300	0.000651
210	0.001075	315	0.000544
225	0.001001	330	0.000507
240	0.000983		

Ambient temperature, °C: 28.
Mass flow rate of air, kg/m^2-s: 1.63.
Mass flow rate of solids, kg/m^2-s: 0.50.
Temperature at the center of the column, °C : 60.
Initial moisture content of solids, kg moisture/kg dry solid: 0.0203.
Average outlet moisture content, ($\bar{c}/c_0$): 0.0439 kg water/kg dry solid.

method and moisture concentration is expressed as kg moisture/kg dry sand. Fig. 1 shows the experimental setup and the baffle plate indicating the solids flow path.

Drying experiments were performed in a single stage continuous fluidized bed dryer using a binary solid mixture of sand containing 20% of coarse size (d_p=0.995 mm) and 80% of fine size (d_p=0.796 mm) under constant drying conditions. Mean particle size of the binary solid mixture is obtained from:

$$d_\mathrm{p} = \frac{1}{\sum_{i=1}^{n} \phi_i / d_{\mathrm{p}i}} \tag{1}$$

where ϕ_i is the mass fraction of i of particle size $d_{\mathrm{p}i}$.
The relative moisture content of the solids in the product is obtained as:

$$\frac{\bar{c}}{c_0} = \frac{\int (c/c_0)dt}{\int dt} \tag{2}$$

Table 1 shows the experimental conditions of the present investigation [2] and the experimental drying data for a typical experiment are shown in Table 2.

3. Artificial neural networks

Artificial Neural Networks have been successfully used in the prediction and optimization problems in Bioprocessing and Chemical Engineering [3]. ANN is a massive parallel-distributed information processing system that has certain performance characteristics resembling biological neural networks of the human brain. ANN has been developed as a generalization of mathematical models of human cognition and neural biology.

The available data set is partitioned into two parts, one corresponding to training and the other corresponding to validation of the model. The purpose of training is to determine the set of connection weights and nodal thresholds that cause the ANN to estimate outputs that are sufficiently close to target values. This fraction of the complete data to be employed for training should contain sufficient patterns so that the network can mimic the underlying relationship between input and output variables adequately. The weights and biases are assigned small random values initially. During training, these are adjusted based on the error or the difference between ANN output and target responses. This adjustment can be continued recursively until a weight space is found, which results in the smallest and overall prediction error. The performance of a trained ANN can be fairly evaluated by subjecting it to new patterns that it has not seen during training. The performance of the network can be determined by computing the percentage error between predicted and desired values.

The network consists of an input layer, an output layer and a number of hidden layers. At each node in a layer the information is received, stored, processed and communicated further to nodes in the next layer. All the weights are initialized to small random numeric values at the beginning of training. These weights are updated or modified iteratively using the generalized delta rule or steepest-gradient descent principle. The training process is stopped when no appreciable change is observed in the values associated with the connection links or some termination criterion is satisfied. Thus, the training of a back-propagation network consists of two phases: a forward pass during which the processing of information occurs from the input layer to the output and a backward pass when the error from the output layer is propagated back to the input layer and the interconnections are modified.

4. Results and discussion

The relative moisture content of solids in the product is calculated using Eq. (2). The following observations have been made based on the experimental data on continuous fluidized bed drying of solids obtained for changes in temperature, inlet solids flow rate, initial moisture content of solids and flow rate of air.

4.1. Effect of temperature

It is seen that drying rate is enhanced with an increase in temperature. It is also observed that the equilibrium moisture content decreases with increase in temperature. Furthermore, the change in drying rate between temperatures 40 °C and 50 °C is more than that between 50 °C and 60 °C. Due to low initial moisture content, an increase in temperature may increase the drying rate but at higher temperatures, its effect over the drying rate may not increase proportionately.

4.2. Effect of inlet solids flow rate

An increase in solids flow rate decreases the mean holding time of solids, which is in agreement with that of Chandran et al. [4]. As the inlet solids flow rate is increased, the rate of drying decreased due to increase in holdup of solids.

4.3. Effect of initial moisture content of solids

It was observed that as the initial moisture content is increased, the equilibrium moisture content also increases. However, the time required to obtain a particular moisture content in the product was found to be more for the solids with high initial moisture content.

4.4. Effect of flow rate of air

With increase in flow rate of air, the drying rate is enhanced.

Outlet moisture content is found to decrease with increase in temperature and decrease in initial moisture content of solids.

Using Tanks-in-series model, Lenin Babu and Pydi Setty [1] developed a kinetic model for drying of solids in a continuous fluidized bed to predict the average moisture content of solids in the product

$$\frac{\bar{c}}{c_0} = \int_0^{\alpha} \left(\frac{c}{c_0}\right)_b E(\theta) d\theta \tag{3}$$

where $E(\theta)$ represents exit age distribution of particles in a continuous dryer.
For a system exhibiting only constant rate period,

$$\frac{\bar{c}}{c_0} = 1 - \frac{R\bar{t}}{c_0} \tag{4}$$

For a system exhibiting only falling rate period,

$$\frac{\bar{c}}{c_0} = 1 - \frac{R}{\beta c_0}\left[1 - \left(\frac{N}{N + \beta\bar{t}}\right)^N\right] \tag{5}$$

The data obtained for the system without baffle [5] are fitted to the drying model obtained using Tanks-in-series model to describe RTD of solids and the results are tabulated for typical experiments by Lenin Babu and Pydi Setty [1], which are shown in Table 3. The table shows the predicted values from the model and the corresponding percentage errors.

Using experimental data in a continuous fluidized bed dryer, ANN models have been developed to predict the outlet moisture content of solids. Two different models have been developed for two separate sets of data. The first data set corresponds to the experiments performed when there is no baffle present [5] whereas the second set is obtained when the vertical baffle is present between the solids inlet and the downcomer [2].

For the first data set, three input variables are chosen, namely, inlet solids flow rate, air flow rate and temperature at the center of the column, whereas for the second set, an additional fourth variable, namely, initial moisture content of solids, is considered. However, in both cases, the output variable is the average outlet moisture content.

Table 3
Results of earlier investigators [1] using tanks-in-series model

S. no	Number of theoretical stages	Experimental average outlet moisture content	Predicted average outlet moisture content	Percentage error
1	5	0.2914	0.2610	10.4170
2	7	0.2673	0.2387	10.7020
3	7	0.2812	0.2484	11.6910
4	10	0.1660	0.1473	11.2770

Table 4
Results obtained from network modeling [5]

S. no	Network output	Desired output	Percentage error
Results of recall of training data			
1	0.3238	0.3235	0.0722
2	0.3056	0.3064	0.2421
3	0.2582	0.2582	0.0101
4	0.2550	0.2547	0.0955
5	0.2380	0.2403	0.9326
6	0.2296	0.2269	1.1743
7	0.2525	0.2528	0.1289
8	0.2840	0.2850	0.3406
9	0.2431	0.2465	1.3755
10	0.2344	0.2333	0.4750
11	0.2769	0.2750	0.6905
12	0.2334	0.2329	0.2177
13	0.2039	0.2060	1.0434
14	0.2090	0.2060	1.4221
15	0.2310	0.2349	1.6459
16	0.2396	0.2371	1.0560
17	0.2029	0.2055	1.2587
18	0.2190	0.2175	0.6809
19	0.2704	0.2673	1.1480
20	0.2812	0.2812	0.0167
21	0.1883	0.1898	0.7774
22	0.1814	0.1814	0.0160
23	0.1740	0.1811	3.9436
24	0.1210	0.1210	0.0089
25	0.1052	0.1000	5.2353
26	0.1094	0.1012	8.0842
27	0.2937	0.2914	0.7875
28	0.1747	0.1760	0.7396
29	0.1366	0.1405	2.7987
30	0.0987	0.1000	1.2567
Results obtained for testing data			
1	0.2906	0.2885	0.7202
2	0.1689	0.1660	1.7482
3	0.2262	0.2430	6.9084
4	0.3035	0.3022	0.4223
5	0.2276	0.2375	4.1743
6	0.3188	0.3222	1.0734
7	0.1750	0.1823	3.9854

Data set: I.
Number of hidden layers: 1.
Input neurons: 3.
Output neuron: 1.
Neurons in the hidden layer: 6.
Activation function used: Sigmoid.
Training algorithm: Back propagation.

Table 5
Results obtained from network modeling [2]

S. no	Network output	Desired output	Percentage error
Results of recall of training data			
1	0.1449	0.1412	2.6283
2	0.0871	0.0855	1.8371
3	0.1279	0.1295	1.2411
4	0.2702	0.2619	3.1564
5	0.0829	0.0797	4.0400
6	0.0873	0.0847	3.0605
7	0.0782	0.0693	12.8660
8	0.2437	0.2409	1.1609
9	0.1569	0.1531	2.5192
10	0.0985	0.0949	3.8226
11	0.1586	0.1554	2.0735
12	0.0908	0.0870	4.2922
13	0.0863	0.0802	7.6556
14	0.0865	0.0866	0.1600
15	0.1210	0.1199	0.9469
16	0.1572	0.1535	2.3912
17	0.0954	0.0907	5.1755
18	0.0716	0.0646	10.8050
19	0.1176	0.1154	1.8808
20	0.0827	0.0774	6.8392
21	0.0782	0.0758	3.1478
22	0.1119	0.1101	1.6380
23	0.1866	0.1842	1.2774
24	0.1163	0.1146	1.4220
25	0.1003	0.0988	1.5824
26	0.1882	0.1833	2.6702
Results obtained for testing data			
1	0.0727	0.0707	2.8825
2	0.0571	0.0578	1.2145
3	0.0866	0.0909	4.7464
4	0.0420	0.0435	3.3459
5	0.1359	0.1314	3.4501

Data set: II.
Number of hidden layers: 2.
Input neurons: 4.
Output neuron: 1.
Neurons in the first hidden layer: 15.
Neurons in the second hidden layer: 10.
Activation function used: Sigmoid.
Training algorithm: Back propagation.

The data set is first normalized and then divided into two parts, one of which is used for training the network and the other for testing. The training procedure continues on an optimal procedure until an optimal architecture is attained. Plotting the model output against the desired response and also evaluating the percentage error between the predicted and desired values assesses the performance of the network. The desired, predicted values and percentage error for the training and testing data for various network architectures are also tabulated in Tables 4 and 5.

5. Conclusions

The resultant network as seen from the above results for the first data set is simple and its performance evaluated by the percentage error criterion is also satisfactory. On the other hand, introducing one more input variable makes the network more complex as seen from the results of the second set. It has been observed that back-propagation networks with two hidden layers outperform the single hidden layer networks when applied to prediction problems.

As seen from Tables 3–5, the average error predicted by the ANN model is less than that predicted by the mathematical model, indicating a better fit of ANN model compared to the usual drying models suggested for drying of solids in a continuous fluidized bed. Also, the network is able to learn the underlying rule even when the training data sets contain noise and measurement errors.

Nomenclature

$c(t)$	Moisture content of solids at any time, kg water/kg dry solid
$\bar{c}$	Average moisture content of solids, kg water/kg dry solid
c_0	Initial moisture content of solids, kg water/kg dry solid
c^+	Equilibrium moisture content of solids, kg water/kg dry solid
d_i	Inside diameter of the column, mm
d_p	Particle diameter, mm
N	Number of stages
R	Constant drying rate, kg water/kg dry solid-s
t	Time, s
t_c	Time corresponding to critical moisture content, s
$\bar{\mathrm{t}}$	Mean residence time, s
β	$\mathrm{R}/(c-\mathrm{c}^+)$, s^{-1}
θ	Dimensionless time, $t/\bar{t}$
θ_c	Dimensionless time corresponding to critical moisture content, $t_\mathrm{c}/\bar{\mathrm{t}}$

References

[1] K. Lenin Babu, Y. Pydi Setty, J. Energy Heat Mass Transf. 23 (2001) 135.

[2] S. Satish, Modeling of a Continuous Fluidized Bed Dryer Using Artificial Neural Networks, M. Tech Thesis, Regional Engg. College, Warangal, 2000.

[3] D.R. Baughman, Y.A. Liu, Neural Networks in Bio-Processing and Chemical Engineering, Academic Press, New York, 1995.

[4] A.N. Chandran, S. Subba Rao, Y.B.G. Varma, AIChE J. 36 (1) (1990) 29.

[5] K. Lenin Babu, Drying of Solids in a Continuous Fluidized Bed, M. Tech Thesis, Regional Engg. College, Warangal, 1999.